Journal of
Information Systems Engineering
and Business Intelligence

Vol.9, No.2, October 2023
Available online at: http://e-journal.unair.ac.id/index.php/JISEBI

A Fast and Reliable Approach for COVID-19 Detection from CT-Scan Images

Md. Jawwad Bin Zahir [1)*], Muhammad Anwarul Azim [2)], Abu Nowshed Chy [3)], Mohammad Khairul Islam [4)]

[1)2)3)4)] *Department of Computer Science and Engineering, University of Chittagong, Chittagong, Bangladesh.*
[1)] jawwad.cse@std.cu.ac.bd, [2)] azim@cu.ac.bd, [3)] nowshed@cu.ac.bd, [4)] mkislam@cu.ac.bd

Abstract

Background: COVID-19 is a highly contagious respiratory disease with multiple mutant variants, an asymptotic nature in patients, and with potential to stay undetected in common tests, which makes it deadlier, more transmissible, and harder to detect. Regardless of variants, the COVID-19 infection shows several observable anomalies in the computed tomography (CT) scans of the lungs, even in the early stages of infection. A quick and reliable way of detecting COVID-19 is essential to manage the growing transmission of COVID-19 and save lives.
Objective: This study focuses on developing a deep learning model that can be used as an auxiliary decision system to detect COVID-19 from chest CT-scan images quickly and effectively.
Methods: In this research, we propose a MobileNet-based transfer learning model to detect COVID-19 in CT-scan images. To test the performance of our proposed model, we collect three publicly available COVID-19 CT-scan datasets and prepare another dataset by combining the collected datasets. We also implement a mobile application using the model trained on the combined dataset, which can be used as an auxiliary decision system for COVID-19 screening in real life.
Results: Our proposed model achieves a promising accuracy of 96.14% on the combined dataset and accuracy of 98.75%, 98.54%, and 97.84% respectively in detecting COVID-19 samples on the collected datasets. It also outperforms other transfer learning models while having lower memory consumption, ensuring the best performance in both normal and low-powered, resource-constrained devices.
Conclusion: We believe, the promising performance of our proposed method will facilitate its use as an auxiliary decision system to detect COVID-19 patients quickly and reliably. This will allow authorities to take immediate measures to limit COVID-19 transmission to prevent further casualties as well as accelerate the screening for COVID-19 while reducing the workload of medical personnel.

Keywords: Auxiliary Decision System, COVID-19, CT Scan, Deep Learning, MobileNet, Transfer Learning

Article history: Received 30 July 2023, first decision 29 September 2023, accepted 27 October 2023, available online 28 October 2023

I. INTRODUCTION

Coronavirus disease 2019 (COVID-19) is a highly contagious respiratory illness caused by a virus named severe acute respiratory syndrome coronavirus 2 or SARS-CoV-2, which has claimed more than 6.5 million human lives worldwide [1]. Upon entering the respiratory system, the virus causes viral sepsis, which induces severe respiratory distress or pneumonia in the patients. It also destroys the lung cells gradually, which in turn may lead to death by respiratory failure. COVID-19 transmissions occur primarily via respiratory droplets from coughs and sneezes. The affected show initial symptoms like cough, high fever, severe fatigue, muscle spasms, shortness of breath, vomiting, and loss of taste and smell [2]. These initial symptoms of COVID-19 are somehow similar to the symptoms of seasonal flu or community-acquired pneumonia. This makes detecting COVID-19 by symptoms difficult. Furthermore, a significant number (about 40.5% globally [3]) of people who are infected do not develop noticeable symptoms making COVID-19 harder to detect [4], [5]. Nowadays, the multiple mutations of the SARS-CoV-2 virus have also made the disease more deadly and even harder to detect by current means of detection [6].

There are more than five major mutations of the SARS-CoV-2 virus [7], [8]. Among them, the most concerning global variants are the delta and omicron variants. The delta variant that was recorded in October 2020 has significantly increased transmissibility and is more contagious than previous variants. It is 50% more transmissible and 2 times more contagious than the alpha variant, and 225% more transmissible than the original strain from Wuhan [9]. The effectiveness of the vaccines has also decreased against the mutation of the delta variant [10], [11]. It also can escape the immune system due to its mutations. In a study, researchers found the delta variants to infect 74% of patients who were fully vaccinated [12]. This has caused an increase in hospitalizations and resulting

* Corresponding author

ISSN 2443-2555 (online) 2598-6333 (print)
doi: http://dx.doi.org/10.20473/jisebi.9.2.288-304

deaths. The omicron variant that was recorded in November 2021, is also highly transmissible. It is more quickly transmissible than the previous Alpha, Beta, Gamma, and Delta variants. It can multiply in the lung cells 70 times faster than the Delta variant [13]. A mutation of omicron gained the nickname of the "stealth" variant due to a lack of similarity from the original Omicron strain and dissimilarities in the spike protein. This has made the variant hard to detect or track. A patient infected with the omicron variant of COVID-19 can spread the virus to others regardless of vaccination status. It can even cause reinfection in people who have recovered from COVID-19 infection. Although it is highly transmissible and contagious, its symptoms are less fatal than the delta variants [14]. For this, although omicron variants have caused a record number of infections in a short period, the death caused by omicron variants is much lower than the delta variant.

Among the methods being used to diagnose COVID-19 worldwide, reverse transcription polymerase chain reaction (RT-PCR), chest X-ray, and computed tomography (CT) scan are the most accepted practices to screen for COVID-19 infection. Among them, CT scan has superior sensitivity and specificity, better accuracy, and excellent positive and negative predictive value for the diagnosis of COVID-19 compared to RT-PCR [15], [16], and chest X-ray [17], [18]. Moreover, RT-PCR, which was widely used before, fails to detect the newer variants of COVID-19 [19], [20]. RT-PCR also may give negative results in the early stages of infection when the viral load is low whereas, CT scans can show the changes due to COVID-19 from the early stages. CT scans of the chest area can show these small details such as small patches, and opaque shadows in the lungs very clearly and accurately, whereas, in X-rays, the patches seem unclear due to the lower sensitivity of X-ray images. The presence of the enclosing ribcage around the lungs and other noises in the X-ray images also restricts us from seeing the smallest development of COVID-19 in the early stages of infection.

Regardless of variants and mutation, a CT scan of a COVID-19-infected patient shows visible anomalies in the lung from early stages. The radiographic imaging of the chest of an affected person contains multiple, irregular, sub-segmental, or segmental ground-glass density shadows in both lungs. Alternatively, it may contain multiple patchy, or large patches of consolidation in both lungs, with a little grid-like or honeycomb-shaped interlobular septal thickening, especially in the middle and lower lobes [21]. The spread of the observable anomalies depends on the stages of infection. Based on the examination of these opacities in of lungs, the doctor can identify the patients affected by COVID-19. Fig. 1 shows the distinctive feature of COVID-19-infected lungs compared to normal lungs.

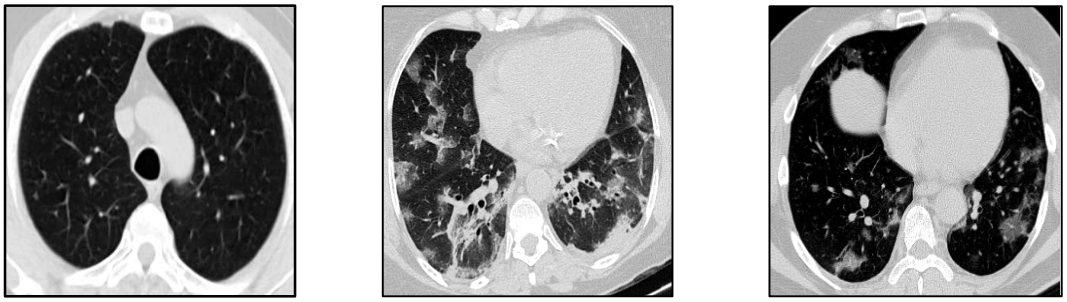

(a) (b) (c)

Fig. 1 Distinctive features of infected lungs. (a) Normal lungs; (b) Infected lungs with ground glass density shadows; (c) Infected lungs with a patch of consolidations

Every day, thousands of people get hospitalized for COVID-19 infection. The limited number of specialized doctors available makes it practically impossible to quickly test, detect, and isolate the growing number of COVID-19 patients. Also, the mutations have made the virus more transmissible and deadlier than before. The damage done to the respiratory system is more severe than the previous infections. There is also the chance of reinfection due to COVID-19 mutations like omicron variants. Normally, the patients are not quarantined until positive results are found on the RT-PCR test. This enables the patients to continue spreading the infection during the conclusion of RT-PCR which is used dominantly in the diagnosis of COVID-19. We need to shorten the time needed for the diagnosis of COVID-19 patients to contain the transmission caused by the mutated variants. Also, we need to detect the infection from its early stages to properly isolate and treat the patients to save their lives. Further, we need to make the process as accessible as possible to properly contribute to the frontline workers for COVID-19. To solve this problem, we need to find a solution that can detect the infection quickly and accurately, so that, we can quickly check and isolate the patients from the early stages of infection to prevent the spread of infection as well as reduce the chance of reinfection in recovering patients.

In this research, we address the problem by automating the detection process using transfer learning to enable quick and accurate detection of infected patients using chest CT scans. We have also created a generalized model that can be used in real life to provide an auxiliary decision system to radiologists in the diagnosis of COVID-19.

We have further demonstrated a way to make the model portable so that it can be used on web-based platforms and mobile devices.

The main objective of this research is to develop an image classification model using transfer learning that can detect CT scans of COVID-19-infected patients quickly, reliably, and accurately. We aim to shorten the time needed to detect a patient with COVID-19 and thus reduce the transmission caused by patients suspected of COVID-19 infection. We also focus on making the model effective so that it can be used in real life as an auxiliary decision system. We further focus on making the model simple, easily trainable as well as accessible to our daily devices.

II. Literature Review

Due to CT scans providing a very clear, accurate, and detailed image of an organ, even before COVID-19, many researchers used images of chest CT scans to detect different diseases such as pneumonia, lung damage, fluid buildup, lung cancer, asthma, etc. in the patients. They have followed different machine learning paradigms to achieve their desired result. During the pandemic, many researchers have come forward and used their prior knowledge and experience to help humanity fight against COVID-19. Some researchers curated multiple sources, collected images of chest CT scans, and labeled them using help from experienced doctors to provide a working dataset to reduce the scarcity of datasets. While others used their knowledge of machine learning on public datasets to automate the detection of COVID-19 in patients.

Yener et al. [22] studied the performance of VGG16 [23], VGG19 [23], and Xception [24] in classifying COVID-19 from CT scans. They have used a balanced dataset with 3227 CT images, which consists of 746 samples from the public dataset provided by Yang et al. [25] along with images they collected from multiple sources from Kaggle [26]. In the research, they used early stopping and reduced learning rate on the plateau with different parameters. They have also applied mini-batching, dropouts, and different learning rates during model training to address overfitting. They achieved the best result using VGG-16 with ImageNet [27] pre-trained weights and a learning rate of 10^{-4}. Their proposed VGG-16 model achieved accuracy of 93%, f1-score of 94% and area under ROC curve 93% in detecting COVID-19 from CT scan images.

Wu et al. [28] compared the performance of AlexNet [29], VGG-16 [23], ResNet [30], SqueezeNet [31], and DenseNet [32] on a small dataset provided by Soares et al. [33] to find the best method of identifying COVID-19 pneumonia in chest CT scan images. They have also tried to determine the effect of pre-trained weights on the performance of the models detecting COVID-19 from CT scan images. They used the pre-training weight of the models trained on the MNIST dataset [34]. Using the pre-trained weights, VGG shows the best accuracy of 80.5% while others show accuracy between 68.5% to 78.5%. Without using the pre-trained weights, only VGG-16 and ResNet models could achieve an accuracy of 82.5% while other models show an accuracy between 70% to 78%. They concluded that not using pre-trained weights gives a better result in the case of detecting COVID-19 from CT scan images.

Anwar et al. [35] fine-tuned EffiecientNet-B4 [36] architecture and trained on the Yang et al. dataset [25] to develop a COVID-19 detector for the CT images. They fined tuned the learning rate of the model. They used three different learning rate strategies. First, they tried reducing the learning rate when model performance stopped increasing. Later they used a cyclic learning rate to train the model. Lastly, they used a constant learning rate to train the model. In the end, they performed 5-fold cross-validation on the test data and averaged the test predictions of each fold to determine which strategy performed better. By comparing the performance, they have determined that the reduce-on-plateau learning rate strategy achieved the best result with an accuracy of 89.7%, an f1-score of 89.6%, and an area under the ROC curve of 89.5%.

Wang et al. [37] modified the InceptionV3 [38] architecture using their curated dataset to establish a COVID-19 detection model. First, they collected images of chest CT scans of pathogen-confirmed COVID-19 cases as well as typical viral pneumonia, totaling 1065 samples. Then, they defined the region of interest in the images, binarized the colors on the image, and reversed the color to highlight the lungs with white and the background with black. After that, they fine-tuned the inception model with pre-trained weight on their curated dataset. While training, they have also used both internal and external validation to improve the performance of the model. The model with internal validation showed the best result with an accuracy of 89.5%, recall or sensitivity of 88%, specificity of 87%, f1-score of 77% and area under ROC curve 93%.

Islam et al. [39] used the LeNet-5 CNN architecture to detect COVID-19 from chest CT scans. The architecture consists of five layers. The first two layers consist of blocks of the convolution layer, followed by one average pooling layer. The next two layers are fully connected layers of sizes 120 and 84 sequentially. The final layer is the output layer with a sigmoid activation function. They trained the architecture on the Yang et al. dataset [25] to evaluate the performance of their model. The highest accuracy of 86.06%, with 85% precision in detecting COVID-19 from CT scans, and an f1 score of 87% was achieved by their proposed model. They also achieved 86% area under the ROC curve using the same.

He et al. [40] proposed a deep learning approach that follows the self-trans approach and combines transfer learning with self-supervised learning to learn the distinctive and unbiased features from the inputs to effectively

detect COVID-19 from CT scan images. Their approach can achieve excellent diagnostic accuracy even with a limited number of training samples, making it a sample-efficient method. Their method not only captures the underlying patterns and properties of data without using human-annotated labels but also reduces the risk of overfitting. The model learns the distinctive features by creating multiple secondary tasks based on the data itself and forces the network to learn meaningful representations by executing those secondary tasks. Also, they collected CT scan images of COVID-positive patients to build a dataset [25] for their model to be trained on. In their experimental study, they used several training methods with multiple transfer learning models and different initial configurations and then compared the performance with models trained with their self-trans architecture. They demonstrated that models trained with their self-trans method outperform all those other methods trained during the study. Among the models trained on their approach, their self-trans DenseNet-169 architecture achieves the best result with an accuracy of 86%, an f1-score of 85%, and an area under the ROC curve of 94%.

Foysal et al. [41] introduced an ensemble hard voting model that incorporated three independent CNN architectures for accurately classifying the COVID cases. The CNN architectures used three, four, and three convolutional blocks in total respectively. Each block in architecture was followed by a Max Pooling layer. In each architecture, a Batch Normalization layer was used after the first block to enable quick learning of the model. Finally, they trained the ensemble model using the dataset provided by Soares et al. [33]. Their ensemble model achieved an accuracy of 96%, an f1-score of 95.6%, and a recall or sensitivity of 97%.

The research to develop a model to detect COVID-19 from radiographical images mainly focuses on analyzing the implicit graphical features in the images to determine if the patients are suffering from COVID-19. This enables the model to function as an auxiliary decision system to provide a clinical diagnosis ahead of the pathogenic test, thus saving critical time for disease control. From the discussions above, we can see that most of the research fails to show a promising result that will enable it to be used as a secondary decision method. Also, most of the research focuses on a single dataset with a small number of samples. Despite research like Foysal et al. [41] and Yener et al. [22] achieving high accuracy, sensitivity, and F1 scores, the model could have been more generalized and robust if a larger number of samples from varying sources could be used in the training of the model. Moreover, the best results of the ensemble model in Foysal et al. [41] come in a cost of complex model structure and more computational cost. Furthermore, the trained models are bulky in size and cannot be deployed in our daily devices with lower computational power. Also, the complex structural model makes it difficult to reuse the model on other tasks or to be retrained on other samples and have the same kind of performance. In our research, we try to address the shortcomings of the discussed studies and aim to develop a better model with simple architecture, lower training time, higher performance and the ability to be deployed on devices with lower computational power.

III. Methods

A. Dataset Collection

Three different datasets containing images of CT scans are collected for this research. The datasets contain images of varying dimensions collected from multiple different sources. The datasets are used to train our proposed model individually to evaluate the performance of our proposed model on varying sizes of datasets. Finally, we created another dataset by combining all our collected datasets to train the best-performing generalized model to detect COVID-19 from CT scan images. The generalized model is later used as the logical back-end for our mobile application. The number of samples of the datasets used in this research is presented in Table 1.

TABLE 1
SUMMARY OF USED DATASETS

Dataset	COVID	Non-COVID	Total
Yang et al. [25]	349	397	746
Soares et al. [33]	1227	1226	2453
Maftouni et al. [42]	7593	6893	14486
Combined Dataset	8820	8119	16939

The dataset collected by Yang et al. [25] consists of 349 positive COVID-19 samples and 397 negative COVID-19 samples. The dataset was created by collecting CT scan images from papers related to COVID-19 published in medRxiv [43] and bioRxiv [44]. This dataset is used to evaluate the performance of our proposed model when a small amount of sample data is available for training.

The dataset published by Soares et al. [33] contains 1252 CT scans with COVID-19 and 1230 CT scans of non-COVID samples. The CT scans for the dataset were collected from 120 patients in different hospitals in Sao Paulo, Brazil. For this research, we modified the original dataset by examining all CT scan images and removing the samples where the lung is not properly visible in the image. The modified dataset contains only 1227 COVID-19 samples and 1226 non-COVID samples. This dataset is used by many researchers. So, this dataset was used to evaluate our model to validate how our proposed model performs against the proposed model of other researchers.

The dataset published by Maftouni et al. [42] is a compilation of multiple public datasets [25], [45]–[50]. The original dataset contains 7593 COVID samples, 6893 non-COVID samples, and 2618 Community-Acquired Pneumonia (CAP) samples. For this research, we have modified the dataset by removing the CAP samples from the dataset. The modified dataset contains only 7593 COVID samples and 6893 non-COVID samples. This model is used in research to check how our model performs on a large amount of data collected from heterogeneous sources.

We created a new dataset by combining all our collected datasets. Yang et al. [25] dataset is already included in the Maftouni et al. [42] dataset. So, our dataset is created by combining only the samples in the modified Soares et al. dataset [33] and Maftouni et al. [42] dataset. The dataset contains a total of 8820 COVID-19 samples and 8119 non-COVID samples. The dataset is a balanced dataset with a ratio of 52:48 for COVID and non-COVID samples respectively. This dataset is used to train our generalized model which can be used in real life.

B. Model Architecture Selection

1) Model Selection

Normally, vision-related services are provided for internet-connected devices through cloud infrastructures for their superior processing power and higher storage capacity. In this research, we aim to make our model accessible to as many people as possible so that it can be used to properly control the rampant transmission of COVID-19 variants. Therefore, we have to train a model that not only provides the best performance in a normal environment but also on low-powered, resource-constrained devices. To achieve this, our proposed model must be able to run quickly with the highest performance and reliability while being small in size and requiring less computational power. For this reason, we use MobileNet [51] as our transfer learning model for our proposed architecture.

MobileNet is a small, efficient, low-latency, low-power transfer learning model parameterized to meet the resource constraints of a variety of use cases. It uses depth-wise separable convolutions instead of the traditional convolution layer which significantly reduces the number of parameters when compared to the transfer learning models with regular convolutions with the same depth. This enables MobileNet to be simple and efficient while being lightweight and less computation intensive.

Depth-wise separable convolution layers perform two consecutive operations, i.e., the depth-wise convolution and the point-wise convolution. Depth-wise convolution applies a single filter into each input channel contrary to standard convolution which applies filters on all input channels. Pointwise convolution computes a linear combination of the output of depth-wise convolution using a 1 × 1 convolution layer. Depth-wise separable convolution layers use depth-wise convolution to filter the input channels and then use pointwise convolution to combine them to create a new feature. This consecutive use of these two operations enables depth-wise separable convolution layers to require a 9 times smaller number of multiplications than that of standard convolution layers. Fig. 2 shows the structure of the depth-wise separable convolution layer compared to the standard convolution layer. Fig. 3 shows the architecture of MobileNet utilizing the depth-wise separable convolution layers.

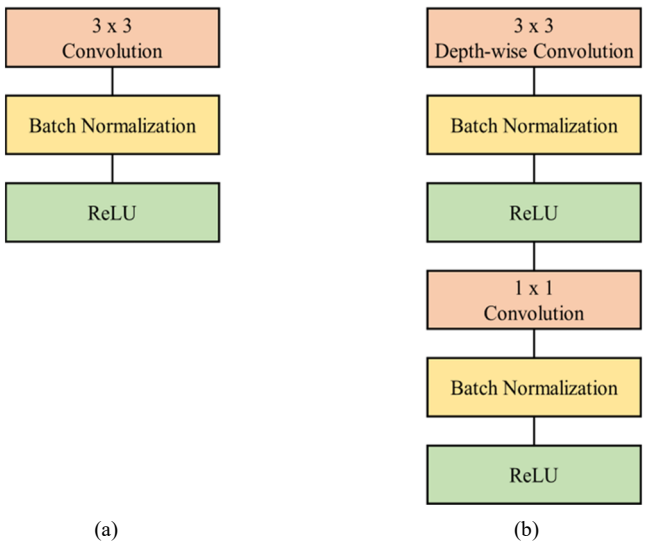

Fig. 2 Convolution layer structures. (a) Standard convolution layer; (b) Depth-wise separable convolution layer

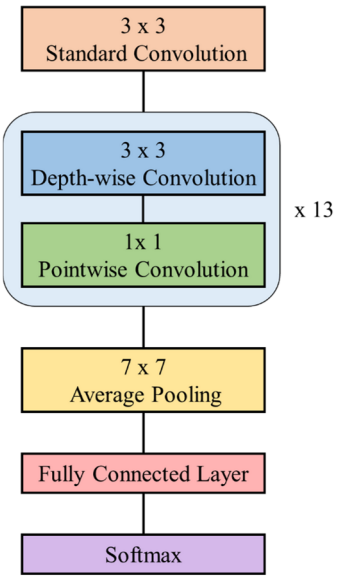

Fig. 3 MobileNet architecture

2) Proposed Architecture

The architecture of the proposed model architecture consists of two main units, namely, the preprocessing unit and the transfer learning unit. The preprocessing unit loads the CT scan images and preprocesses them to meet the input requirements for the image classification. The transfer learning unit extracts unique features from the images, calibrates the models, and uses the extracted knowledge to differentiate between chest CT scan images of normal and COVID-19-infected patients. The proposed model architecture is mentioned as COVID-CT-Net henceforth in this paper. Fig. 4 shows the overall structure and components of the proposed model architecture.

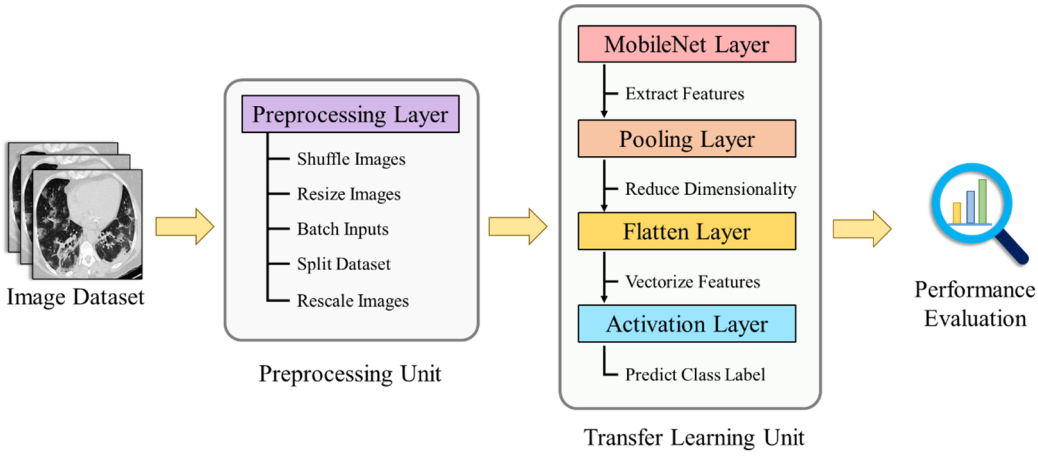

Fig. 4 Overview of proposed COVID-CT-Net architecture

The preprocessing unit contains the preprocessing layer which loads the entire dataset into the workspace and prepares the data according to the requirements of the transfer learning unit. At first, it resizes the image to meet the minimum size requirement of the transfer learning unit. Then it randomly shuffles the images and groups them into multiple batches. Afterward, it splits the batches into training, validation, and test sets. Finally, it rescales the image and normalizes the pixel values of the image to meet the specified value range of inputs for the transfer learning unit.

The transfer learning unit holds the model used in this research. We have modified the original MobileNet architecture to develop the architecture for our proposed model. In COVID-CT-Net architecture, MobileNet only acts as a feature extractor for the forthcoming layers. We only use the standard convolution layer and depth-wise separable convolution layers of the original architecture. The other layers present in the architecture are pruned to modify the model for our CT scan images. A max-pooling layer instead of average pooling from the original architecture is used to reduce the spatial dimension of the features. The flatten layer instead of the fully connected layer is used in our model architecture. Finally, a sigmoid function instead of softmax is used as an activation

function to predict the class of the CT scan images. The model architecture for the transfer learning unit is illustrated in Fig. 5.

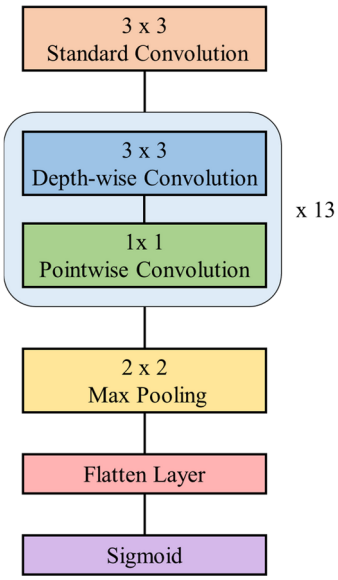

Fig. 4 Proposed model architecture for the transfer learning unit

The MobileNet layer uses the convolutional layers to extract unique features from the images in our training dataset. The unique features are passed to the pooling layer which reduces the dimensionality of the extracted features. The flatten layer vectorizes the feature matrix obtained from the pooling layer by converting the features into a 1-D column vector. Finally, the activation layer uses the vectorized features to predict the class label of the input image.

C. Data Preparation

Data preprocessing is an important step that prepares the input data and makes the data suitable for machine learning models. Data preprocessing not only improves the performance of the model but also reduces the training time.

In this step, we use our preprocessing unit to prepare the data as the input for the transfer learning unit. To make the data compatible with the MobileNet architecture, we keep all 3 channels in the input images although the images are in grayscale. Moreover, we did not use any data augmentation on the images to increase our sample size. The further preprocessing operations performed on the datasets are explained in the following sections and the parameters are summarized in Table 2.

1) Data Cleaning

To remove the inconsistent data from the datasets, we examine the images in the datasets to drop the unsuitable images where the lungs are not properly visible in the CT scan. We also removed the samples irrelevant to our research scope.

2) Input Pipeline Modification

To utilize the full training capability and reduce the model training time drastically, the whole dataset is copied into the virtual machine provided by Google Colab. The dataset is imported into the virtual machine as a zip file and extracted into the current working directory of the virtual machine. Then the dataset is read directly from the current directory and passed into the input layer. This modification removes the bottleneck process of individually reading the data from Google Drive every time the data is needed. For example, this modification reduces the training time for the Soares et al. [34] dataset from 40 minutes to about 6 minutes.

3) Class Label Definition

The class labels have been inferred from the label of the folder where the data is stored. Since we have not modified the folder structure of the used datasets, the original labels for the classes defined by the respective dataset authors have become the class labels for the data in that particular dataset.

4) Dimensionality Reduction

The dimension of the images in the dataset ranges from 115×98 to 1858×1275. But, to get the best performance, the images passed to the model need to have the same dimension. To address this issue, we have modified the dimensionality of the images to 224×224 pixels, so that every image passed to the model matches the dimension of the images the transfer model is trained on. We have used the lossy compression method to achieve this. Also, no region has been cropped from the image in this process.

5) Data Normalization

The transfer learning models are trained on the ImageNet [55] dataset and the input to the transfer learning models also needs to match the image intensity range of the ImageNet dataset. So, we have normalized the image intensity from the range [0, 255] to [-1, 1] to match the image intensity of the samples in the ImageNet dataset.

6) Data Batching

We have randomly shuffled the dataset and distributed it into batches of 32 images per batch.

7) Dataset Splitting

After applying several splitting ratios for training, validation, and test sets on the datasets, we found that the ratio 70:10:20 provides the best result. So, in this research, we have used the ratio 70:10:20 for splitting the dataset into training, validation, and test sets respectively. At first, we reserved 20% of the data in the dataset as a test set, to measure the performance of the model. Then, we used the remaining 80% for training our model. From the remaining 80%, 10% of the data is used as a validation set to address overfitting in the model while training.

TABLE 2
PARAMETERS USED FOR DATA PREPARATION

Parameter	Value
Intensity Range	[-1,1]
Image Dimension	(224,224, 3)
Batch Size	32
Dataset Splitting Ratio	70:10:20

D. Model Implementation

In this research, we used Tensorflow [52] and Keras [53] as the machine learning library and Google Colab [54] as the notebook environment to implement our proposed architecture. We used GPU as the hardware accelerator in google colab for this research. The models discussed in this research were trained with 13 GB of RAM, 15 GB of Tesla T4 GPU, and 2.2 GHz Intel Xeon CPU provided by the free tier of Google Colab.

We implement the transfer learning unit of our COVID-CT-Net model on Google Colab using a sequential model from the Keras library. As the input images for the MobileNet layer are required to have 3 channels, the input shape for the MobileNet layer is set to (224,224,3). The weight pre-trained on the ImageNet dataset is used as the initial weight for our MobileNet layer. As we are using only the depth-wise separable convolutions layers of the MobileNet architecture, including the top fully connected layer at the top of the network is set to False to exclude the fully connected layers of the original MobileNetV1 architecture. This allows us to pass the learned parameter to the next layers and efficiently use the parameters by designing our own fully connected layers for the model. The width multiplier (α) and depth multiplier (ρ) are both set to 1 to utilize the full potential of the depth-wise separable convolutions layers. The dropout for our model is set to 0.001.

The MobileNet layer is followed by a MaxPooling2d layer with a pooling size of (2,2) with no padding and stride equal to the pooling size. The MaxPooling2d layer is followed by a flatten layer and an activation layer with a size of 2 with a sigmoid activation function. Table 3 summarizes the parameters used to implement the transfer learning unit of the COVID-CT-Net model.

TABLE 3
PARAMETERS FOR IMPLEMENTING TRANSFER LEARNING UNIT

Layer	Parameter	Value
MobileNetV1	Input Size	(224,224,3)
	Initial Weight	ImageNet
	Include Top Layers	False
	Width multiplier (α)	1.0
	Depth multiplier (ρ)	1.0
	Dropout	0.001
Max Pooling	Size	(2,2)
	Stride	(2,2)
	Padding	0
Flatten	-	-
Activation	Size	2
	Function	Sigmoid

E. Model Training

The implemented model is executed to extract distinct features from the preprocessed image. The extracted feature is used by the transfer learning unit to classify the CT scan image correctly.

For training the COVID-CT-Net model on collected datasets, we use Adam [55] as an optimizer for the model with a learning rate of 10^{-3}. Categorical cross-entropy is used as a loss function for training the model. The from_logits flag of the loss function is set to True to have more numerical stability of the loss values. The epoch is set to 15 for the model to fit the training data into the model. Table 4 summarizes the parameters used to train the COVID-CT-Net model.

TABLE 4
TRAINING PARAMETERS

Parameter	Value
Optimizer	Adam
Learning Rate	10^{-3}
Loss Function	Categorical Cross-entropy
Epoch	15

We train the COVID-CT-Net model on the collected datasets one by one and evaluate the performance of our model on that dataset. We also save the best-performing models in the SavedModel format of Tensorflow, so that the model and its learned parameters can be reused.

At first, we apply our model to the modified Soares et al. [33] dataset and examine the performance of the proposed model. We also apply other transfer learning models such as DenseNet121, ResNet50V1, VGG16, VGG19, InceptionV3, and Xception as a transfer learning model to demonstrate the comparison between the performance of our COVID-CT-Net with other transfer learning models. We have further compared the performance of our proposed method with the state-of-art models trained on the same dataset.

Later, we apply our model to Yang et al. [25] to check how the model performs on a dataset with a small number of samples. After that, we apply the model to the modified Maftouni et al. [42] dataset to check how the model performs on a larger and more diverse dataset. We also compare the performances with pre-existing models to establish the quality of our proposed model.

Finally, we train the COVID-CT-Net model on our combined CU-COVID-CT dataset, to get a generalized model which can be used in real life. The generalized model is later converted and used as the logical backend for our mobile application.

F. Model Evaluation

After training the models on the training dataset, we evaluate the performance of our proposed model on its ability to detect COVID-19-positive CT scan images from the test dataset. We use several performance measures to analyze the performance of our COVID-CT-Net model. They are Accuracy, Recall, Precision, F1-score, and Area Under the ROC Curve (AUC-ROC). Among them, accuracy, recall, precision, and f1-score are calculated from the confusion matrix, whereas, AUC is calculated as the area under the Receiver Operating Characteristics (ROC) curve in the plot where the True Positive Rate (TPR) on the y-axis and the False Positive Rate (FPR) on the x-axis. Accuracy, Precision, Recall, and F1-score is calculated using equation (1), (2), (3) and (4) respectively.

$$\text{Accuracy} = \frac{\text{Number of COVID}-19\text{ Samples Predicted Correctly}}{\text{Total Number of Samples}} \quad (1)$$

$$\text{Precision} = \frac{\text{Number of Samples Correctly Predicted as Positive}}{\text{Total Number of Samples Predicted as Positive}} \quad (2)$$

$$\text{Recall} = \frac{\text{Number of Samples Correctly Predicted as Positive}}{\text{Total Number of Positive Samples in Dataset}} \quad (3)$$

$$\text{F1} - \text{score} = \frac{2 \times \text{Precision} \times \text{Recall}}{\text{Precision} + \text{Recall}} \quad (4)$$

G. Model Conversion

The saved model generated using TensorFlow [52] is bulky in size as well as contains multiple API calls. So, the models cannot be directly imported into a mobile application to be used in real life. To solve this problem, the saved model is converted into a small-sized TFLite Flatbuffer format. The TFLite model contains the model's execution graph. This can be easily loaded into the memory of a mobile device and necessary operations to detect the COVID-19 samples can be performed as in the SavedModel. The conversion can be done easily using the convert function provided by Tensorflow Lite. We can get a TFLite model by writing the bytes generated by the converter into a file.

The saved model generated by TensorFlow not only contains the weight for the model but also metadata about model input and outputs. However, the model generated by the TensorFlow lite converter does not contain that metadata. To solve this, a metadata populator is used to generate the required metadata for the model. The generated metadata contains information about input size, input pixel value range, input color channel, output

labels, minimum and maximum output level, model author, model license, etc. Finally, the converted model file and the metadata is packed into one file, which can be easily used for making auxiliary decision system for low-powered devices such as smartphones and raspberry pie.

H. Mobile Application Development

Using the TFLite model of the generalized method, we implement a proof-of-concept auxiliary decision system for the Android operating system using Android Studio as the development environment. We have used XML for developing the front end, and Java for implementing the application.

We have used the TFLite flatbuffer model of the COVID-CT-Net model instead of the original SavedModel to further reduce the size of the model and required processing for decisions in the application. Reading the TFLite flatbuffer model, pre-processing the input, and making decisions using the COVID-CT-Net model will be handled within the application. The application will read the metadata of the COVID-CT-Net TFLite flatbuffer model, preprocess the image accordingly, and pass it to our model to classify the image. The model will then read the image and classify it accordingly along with confidence for the decision.

IV. RESULTS

COVID-CT-Net has shown impressive results in all the datasets. When applied to the modified Soares et al. [33] dataset, COVID-CT-Net shows an accuracy of 98.54% in distinguishing COVID-19-infected CT scans from non-COVID ones. Later, applying COVID-CT-Net to the Yang et al. [25] dataset, we achieved a testing accuracy of 98.75% on the dataset. Further applying the COVID-CT-Net model to the Maftouni et al. [42] dataset, we achieved an accuracy of 97.84% in distinguishing the non-COVID samples from the COVID ones. Finally, applying COVID-CT-Net to the combined dataset, we get an excellent performance of 96.14% accuracy in distinguishing COVID-19-infected CT scans from non-COVID ones. Fig. 6 shows the confusion matrices for all the datasets used in the research. Table 5 shows the performance of COVID-CT-Net on the datasets using the evaluation parameters. The ROC curves for all the datasets used in the research are illustrated in Fig. 7.

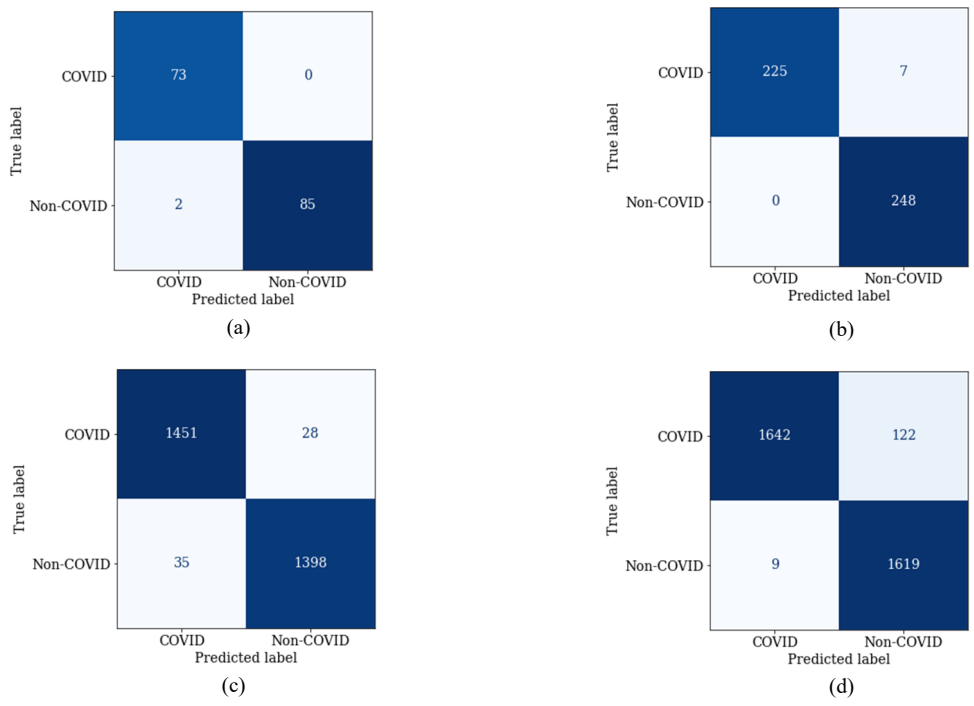

Fig. 5 Confusion Matrix for (a) Yang et al. [25]; (b) Soares et al. [33]; (c) Maftouni et al. [42]; (d) Combined Dataset

TABLE 5
PERFORMANCE OF COVID-CT-NET ON USED DATASETS

Dataset	Accuracy	Precision	Recall	F1 Score	AUC
Yang et al. [25]	98.75%	97.33%	100.00%	98.65%	98.85%
Soares et al. [33]	98.54%	100.00%	96.98%	98.47%	98.49%
Maftouni et al. [42]	97.84%	98.04%	97.56%	97.80%	97.83%
Combined Dataset	96.14%	99.46%	93.08%	96.16%	96.27%

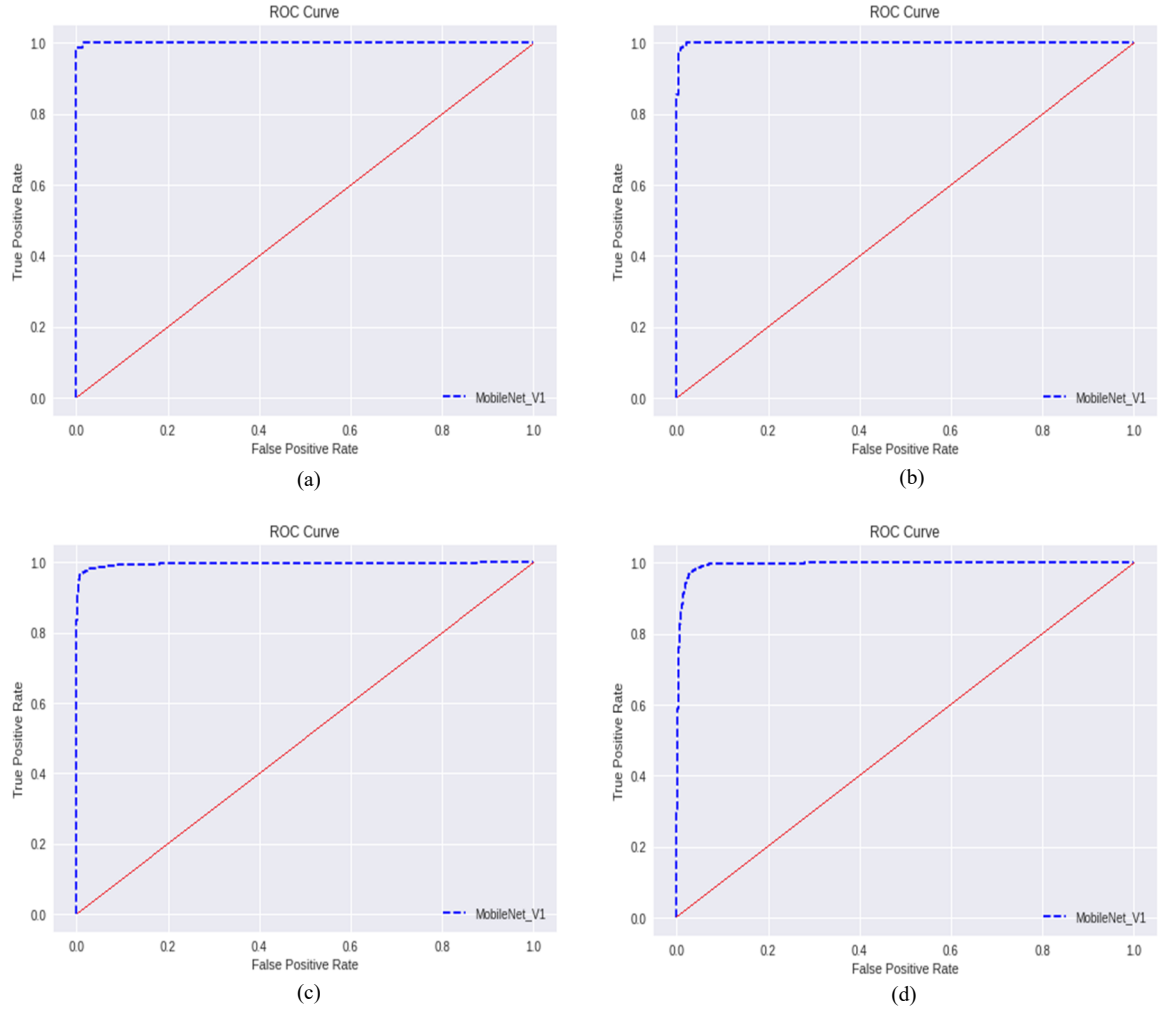

Fig. 6 ROC Curve for (a) Yang et al.; (b) Soares et al.; (c) Maftouni et al.; (d) Combined Dataset

In the receiver operating characteristic curve or ROC curves, the blue line represents the ROC curve of COVID-CT-Net for different classification thresholds, whereas the red line refers to the ROC curve of no separability. The ROC curve for COVID-CT-Net is far above the ROC curve of no separability and the area under the curve (AUC) is very close to the ideal AUC of 100%. Thus, we can say that our COVID-CT-Net not only shows remarkable results but also can exceptionally distinguish between COVID and non-COVID samples.

The proof-of-concept also mobile application shows promising performance as an auxiliary decision system to detect COVID-19 from CT scan images. Despite being only 12 MB in the TFLite model, the model behind the application shows the same performance as our original COVID-CT-Net generalized model.

The mobile application works in the following way as an auxiliary decision system to detect COVID-19 from CT scan images. Fig. 8 demonstrates the process through screenshots of the interface from our mobile application.

1. The user opens the mobile application using the application icon. The application greets the user with a welcome screen.
2. The user is shown the start page of the application with a “Load Image” button. The user presses the “Load Image” button.
3. The user is taken to the gallery to select the image from the device. The user selects the picture.
4. The user is taken to the image analysis page in the application. The user is shown the selected image along with the button “Analyze Image” and “Clear Selection”.
5. If the user presses the “Analyze Image” button, the application will preprocess and analyze the selected image using the TFlite flatbuffer COVID-CT-Net model and show the result on the result page. The application will discard the selected picture and take the user back to the start page if the user presses the “Clear Selection” button.
6. The result page will show the selected image with either "COVID: POSITIVE" or "COVID: NEGATIVE" as a result along with the confidence of the shown result and a button “Check Another”.
7. Selecting “Check Another” will take the user to the start page.

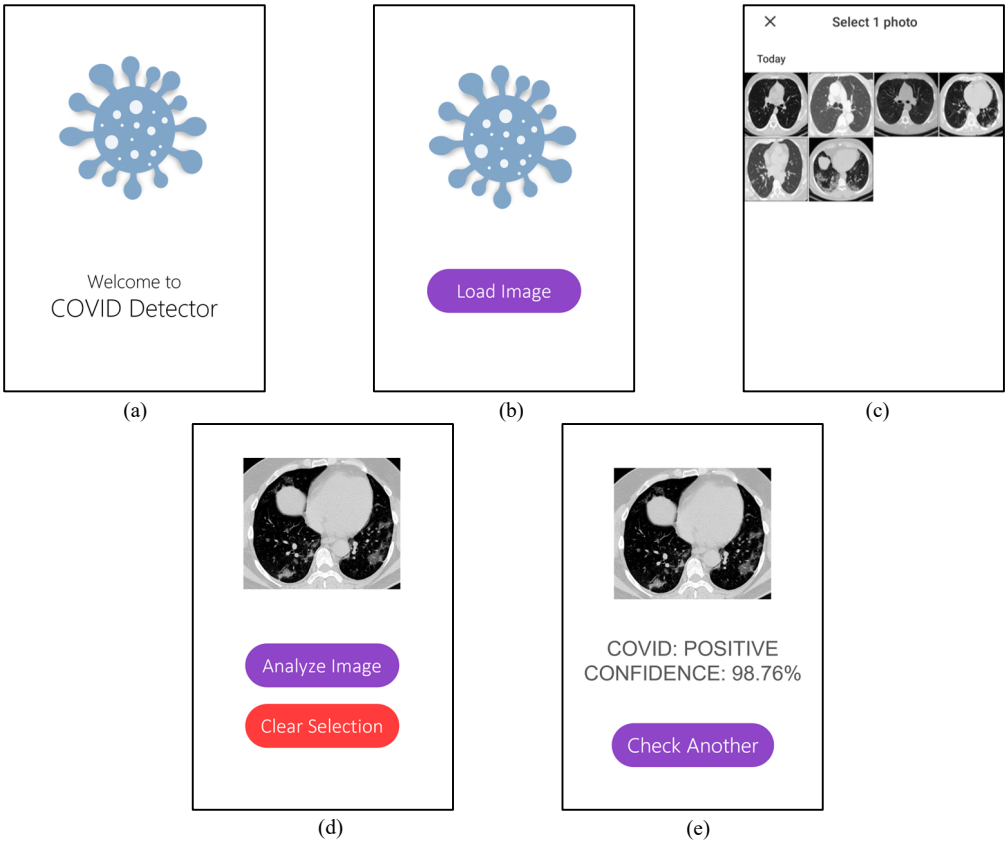

Fig. 7 Mobile Application Screenshots. (a) Welcome Page; (b) Start Page; (c) Image Selection Page; (d) Image Analysis Page; (e) Result Page

V. Discussion

Our proposed COVID-CT-Net shows an impressive performance on all the datasets collected for this research. Our COVID-CT-Net model not only performs remarkably on small datasets like the Yang et al. [25] dataset but also on datasets with a large number of samples such as the Maftouni et al. [42] and the combined dataset. It also handles excellently the varying size of the inputs. Also, the datasets are a curation of samples collected from different sources. The collected images have varying conditions such as brightness, contrast, and cropping. Yet our proposed model has shown promising performance in distinguishing them effectively. So, we believe our COVID-CT-Net can be used as a general model to identify COVID-19 in patients' CT scans as an auxiliary decision system.

To further demonstrate the performance of our proposed model, we have also compared the performance with other results and methods using the same datasets. We have also compared the performance with other transfer learning models in terms of training time, model performance, parameter size, and model size to demonstrate the efficiency of our proposal.

A. Performance Analysis

From the confusion matrix of the generalized COVID-CT-Net model trained on the combined dataset, we can see that the model fails to identify 122 of the total 1764 COVID samples and 9 out of 1628 of the non-COVID samples from the test dataset. Moreover, we can see from the performance matrices that our model has a precision of 99.46% but a recall of 93.08%. That means, our model is correct 99.46% time when it labels a CT image as COVID, but it fails to label 6.92% of the COVID samples of the test COVID samples. So, our generalized model has an error rate of 6.92% for COVID samples and 0.55% for non-COVID samples. The precision value also indicates that our model generates fewer false negatives, which is essential to prevent the spread of different variants of COVID-19 due to unsuspecting and asymptotic COVID-19-infected patients.

B. Comparison with Transfer Learning Models

Using the Soares et al. [33] dataset, we have trained other transfer learning models such as DenseNet121, ResNet50V1, VGG16, VGG19, InceptionV3, and Xception with the same resource and running configuration as our COVID-CT-Net model. Comparing the performances, we can see that, our COVID-CT-Net not only outperforms those models but also has fewer parameters and reduced model size. Moreover, our model has less

training time than those models. So, we can conclude that, despite having a simple architecture, low training time, and smaller model size our model is more efficient in detecting COVID-19 from CT scan images than other transfer learning methods. Table 6 shows the performance comparison with other transfer learning models in detecting COVID-19 from CT scan images. Table 7 compares the model in the aspect of model size and the number of parameters which is essential for deploying the model on low-powered devices.

TABLE 6
PERFORMANCE COMPARISON WITH OTHER TRANSFER LEARNING MODELS

Model	Training Time	Accuracy	Precision	Recall	F1 Score	AUC
COVID-CT-Net	**6m 30s**	**98.54%**	**100.00%**	**96.98%**	**98.47%**	**98.49%**
DenseNet121	13m	82.50%	99.39%	66.40%	79.61%	82.98%
ResNet50V1	11m 20s	90.63%	85.99%	96.60%	90.98%	90.75%
VGG16	13m 20s	90.63%	90.48%	90.09%	90.28%	90.61%
VGG19	15m 20s	88.54%	85.31%	94.44%	89.64%	88.23%
InceptionV3	16m 50s	94.58%	97.47%	92.03%	94.67%	94.71%
Xception	34m 30s	96.04%	99.12%	92.98%	95.95%	96.07%

TABLE 7
MEMORY UTILIZATION COMPARISON WITH OTHER TRANSFER LEARNING MODELS

Model	Total Parameters (Million)	Saved Model Size (MB)
COVID-CT-Net	**3.247**	**40**
DenseNet121	7.055	92
ResNet50V1	23.624	276
VGG16	14.723	170
VGG19	20.033	230
InceptionV3	21.868	259
Xception	20.963	244

C. Comparison with Other Methods and Results

Despite having a simple architecture and low training time, our COVID-CT-Net architecture performs better than other methods used on the datasets used in this research. Moreover, the same configuration of the model provides the best result for all the datasets despite having different numbers of diverse samples. It also surpasses the baseline methods provided by the dataset authors in their paper.

Yang et al. [25] proposed the self-supervising DenseNet-169 architecture [40] as the baseline method having an accuracy of 86% in detecting COVID-19 from CT-scan images. Soares et al. [33] proposed a baseline method using an explainable deep neural network (xDNN) having an accuracy of 97.38%. Whereas, Maftouni et al. [42] trained the baseline model using an ensemble learning approach which showed an accuracy of 95.31% in distinguishing between COVID and non-COVID samples. The comparison between the performance of COVID-CT-Net and the baseline methods is presented in Table 8.

TABLE 8
PERFORMANCE COMPARISON WITH BASELINE RESULTS

Dataset	Model	Accuracy	Precision	Recall	F1 Score	AUC
Yang et al. [25]	COVID-CT-Net	**98.75%**	**97.33%**	**100.00%**	**98.65%**	**98.85%**
	DenseNet-169	86.00%	-	-	85.00%	94.00%
Soares et al. [33]	COVID-CT-Net	**98.54%**	**100.00%**	**96.98%**	**98.47%**	**98.49%**
	xDNN	97.38%	99.16%	95.53%	97.31%	97.36%
Maftouni et al. [42]	COVID-CT-Net	**97.84%**	**98.04%**	**97.56%**	**97.80%**	97.83%
	Ensemble Learning	95.31%	97.93%	90.80%	94.23%	**98.06%**

Many other researchers have used the datasets to develop a method to detect COVID-19 from CT-scan images. Some have used different deep learning or transfer learning methods. Others have tuned the parameters of existing models to get their desired results. Table 9 shows the performance comparison with other methods for Yang et al., Soares et al., and Maftouni et al. dataset sequentially. Comparing the performance with other methods using the same datasets used in our research we have found that our COVID-CT-Net outperforms them by a noteworthy margin.

TABLE 9
PERFORMANCE COMPARISON WITH OTHER METHODS

Dataset	Author(s)	Model	Accuracy	F1 Score
Yang et al. [25]	Our Model	COVID-CT-Net	**98.75%**	**98.65%**
	Yener et al. [22]	VGG16	93.00%	92.00%
	Anwar et al. [35]	EffiecientNet-B4	89.70%	89.60%
	Islam et al. [39]	LeNet-5 CNN	86.06%	87.00%
Soares et al. [33]	Our Model	COVID-CT-Net	**98.54%**	**98.47%**
	Wu et al. [28]	VGG16, ResNet	82.50%	-
	Foysal et al. [41]	Ensembled CNN	96.00%	95.60%
	Panwar et al. [56]	Modified VGG19	95.00%	95.00%
Maftouni et al. [42]	Our Model	COVID-CT-Net	**97.84%**	**97.80%**
	Dhruv et al. [57]	InRFNet	96.00%	96.33%
	A. Ouahab [58]	CNN	88.30%	88.50%
	Hartono at al. [59]	LeNet-5	83.33%	84.89%

VI. CONCLUSIONS

COVID-19 is a respiratory disease that appeared on December 19, 2019, and caused worldwide transmission expeditiously, resulting in the COVID-19 pandemic. It has claimed numerous human lives by inducing severe respiratory distress and damage to the lung cells. Although worldwide governments and doctors are doing an excellent job keeping this disease under control, the recurring appearance of newer variants of the disease is making the containment process difficult. The recurring mutation of COVID-19 has made the disease more transmissible as well as deadly, resulting in a sudden increase in infections, hospitalizations, and even deaths. Moreover, the time needed for detecting COVID-19 with RT-PCR tests, which are being used predominantly around the world, is causing more and more transmissions through unsuspecting patients in the early stages of COVID-19 infection. Some variants are also causing retransmission in recovered patients. To solve this problem, we need a reliable way to detect COVID-19 from patients quickly and effectively to overcome the rampant transmission of COVID-19.

In this research, we have proposed a deep learning model named COVID-CT-Net to detect COVID-19 from images of lung CT scans reliably and efficiently. We have collected three publicly available datasets provided by Soares et al. [33], Yang et al. [25], and Maftouni et al. [42] for this research. We have also created a dataset by curating, preprocessing, and combining the collected datasets to generate a generalized model that can be used as an auxiliary decision system for the radiologist. We have also developed a mobile application as a proof-of-concept using the generalized COVID-CT-Net model to further demonstrate our performance in detecting COVID-19 from CT scan images in low-powered and resource-constrained environments. Despite having a small size, simple architecture, and lower training time, the COVID-CT-Net model has shown astounding accuracy of 98.54%, 98.75%, and 97.84% respectively on the Soares et al. dataset [33], Yang et al. dataset [25], and Maftouni et al. dataset [42] in detecting COVID-19 from CT scan images, outperforming not only other transfer learning models but also state-of-the-art models trained on those datasets. Our generalized COVID-CT-Net model has also shown an excellent performance of 96.14% in detecting COVID-19 from CT scan images. Furthermore, our mobile application has also shown performance similar to the used generalized model despite having a smaller-sized model. Considering the promising performance of our COVID-CT-Net model, we believe that our model will be useful as an auxiliary decision system for detecting COVID-19 from CT scan images which will not only reduce the time needed to diagnose the COVID-19 to a minimum but also help mitigate the risk of transmission and retransmission. We also believe our research will contribute towards overcoming the COVID-19 pandemic, therefore saving the lives of millions of people.

Although our research provides a quick and reliable way to detect COVID-19 from CT scan images, we believe our work can be further expanded in many ways. In the future, we want to use the knowledge from error analysis to make the model more efficient. Additionally, we want to utilize callbacks and data augmentation techniques to make the model more robust and reliable in real-life scenarios. We also want to enable our model to distinguish between the changes in CT scans because of COVID-19 and other types of pneumonia. Furthermore, we want to expand this research to be able to not only detect COVID-19 but also calculate the level of lung damage by assessing the shadows utilizing the excellent sensitivity and clear imaging of CT scans.

Author Contributions: *Md. Jawwad Bin Zahir*: Conceptualization, Methodology, Software, Visualization, Writing - Original Draft. *Muhammad Anwarul Azim*: Supervision, Resources, Project Administration, Writing – Review & Editing. Abu Nowshed Chy: Methodology, Writing – Review & Editing. *Mohammad Khairul Islam*: Conceptualization, Writing – Review & Editing.

All authors have read and agreed to the published version of the manuscript.

Funding: This research received no specific grant from any funding agency.

Conflicts of Interest: The authors declare no conflict of interest.

Data Availability: Datasets used in the manuscript are publicly available in the following repositories:
Yang et al. : https://github.com/UCSD-AI4H/COVID-CT
Soares et al. : https://www.kaggle.com/datasets/plameneduardo/sarscov2-ctscan-dataset
Maftouni et al. : https://www.kaggle.com/datasets/maedemaftouni/large-covid19-ct-slice-dataset
Combined : https://github.com/JawwadSeemanta/COVID-CT-Net_Dataset

Informed Consent: There were no human subjects.

Animal Subjects: There were no animal subjects.

ORCID:
Md. Jawwad Bin Zahir: https://orcid.org/0000-0003-4920-5560
Muhammad Anwarul Azim: https://orcid.org/0000-0001-6315-3950
Abu Nowshed Chy: https://orcid.org/0000-0001-6044-842X
Mohammad Khairul Islam: https://orcid.org/0000-0001-5432-1406

REFERENCES

[1] World Health Organization (WHO), "WHO Coronavirus (COVID-19) Dashboard." https://covid19.who.int (accessed Jul. 07, 2023).

[2] "Clinical characteristics of COVID-19," *European Centre for Disease Prevention and Control*. https://www.ecdc.europa.eu/en/covid-19/latest-evidence/clinical (accessed Jan. 14, 2022).

[3] Q. Ma *et al.*, "Global Percentage of Asymptomatic SARS-CoV-2 Infections Among the Tested Population and Individuals With Confirmed COVID-19 Diagnosis: A Systematic Review and Meta-analysis," *JAMA Netw. Open*, vol. 4, no. 12, p. e2137257, Dec. 2021, doi: 10.1001/jamanetworkopen.2021.37257.

[4] B. Nogrady, "What the data say about asymptomatic COVID infections," *Nature*, vol. 587, no. 7835, pp. 534–535, Nov. 2020, doi: 10.1038/d41586-020-03141-3.

[5] D. P. Oran and E. J. Topol, "The Proportion of SARS-CoV-2 Infections That Are Asymptomatic: A Systematic Review," *Ann. Intern. Med.*, vol. 174, no. 5, pp. 655–662, May 2021, doi: 10.7326/M20-6976.

[6] "SARS-CoV-2 Viral Mutations: Impact on COVID-19 Tests," *FDA*, Dec. 2021, Accessed: Mar. 26, 2023. [Online]. Available: https://www.fda.gov/medical-devices/coronavirus-covid-19-and-medical-devices/sars-cov-2-viral-mutations-impact-covid-19-tests

[7] "Tracking SARS-CoV-2 variants." https://www.who.int/activities/tracking-SARS-CoV-2-variants (accessed Jan. 11, 2023).

[8] "SARS-CoV-2 Variant Classifications and Definitions," *Centers for Disease Control and Prevention*, Feb. 11, 2023. https://www.cdc.gov/coronavirus/2019-ncov/variants/variant-classifications.html (accessed Jan. 01, 2023).

[9] E. Callaway, "The mutation that helps Delta spread like wildfire," *Nature*, vol. 596, no. 7873, pp. 472–473, Aug. 2021, doi: 10.1038/d41586-021-02275-2.

[10] A. Fowlkes, "Effectiveness of COVID-19 Vaccines in Preventing SARS-CoV-2 Infection Among Frontline Workers Before and During B.1.617.2 (Delta) Variant Predominance — Eight U.S. Locations, December 2020–August 2021," *MMWR Morb. Mortal. Wkly. Rep.*, vol. 70, 2021, doi: 10.15585/mmwr.mm7034e4.

[11] J. Lopez Bernal *et al.*, "Effectiveness of Covid-19 Vaccines against the B.1.617.2 (Delta) Variant," *N. Engl. J. Med.*, vol. 385, no. 7, pp. 585–594, Aug. 2021, doi: 10.1056/NEJMoa2108891.

[12] C. M. Brown, "Outbreak of SARS-CoV-2 Infections, Including COVID-19 Vaccine Breakthrough Infections, Associated with Large Public Gatherings — Barnstable County, Massachusetts, July 2021," *MMWR Morb. Mortal. Wkly. Rep.*, vol. 70, 2021, doi: 10.15585/mmwr.mm7031e2.

[13] V. Papanikolaou *et al.*, "From delta to Omicron: S1-RBD/S2 mutation/deletion equilibrium in SARS-CoV-2 defined variants," *Gene*, vol. 814, p. 146134, Mar. 2022, doi: 10.1016/j.gene.2021.146134.

[14] J. A. Lewnard, V. X. Hong, M. M. Patel, R. Kahn, M. Lipsitch, and S. Y. Tartof, "Clinical outcomes associated with SARS-CoV-2 Omicron (B.1.1.529) variant and BA.1/BA.1.1 or BA.2 subvariant infection in Southern California," *Nat. Med.*, vol. 28, no. 9, Art. no. 9, Sep. 2022, doi: 10.1038/s41591-022-01887-z.

[15] T. Ai *et al.*, "Correlation of Chest CT and RT-PCR Testing for Coronavirus Disease 2019 (COVID-19) in China: A Report of 1014 Cases," *Radiology*, vol. 296, no. 2, pp. 32–40, 2020, doi: 10.1148/radiol.2020200642.

[16] A. Dangis *et al.*, "Accuracy and Reproducibility of Low-Dose Submillisievert Chest CT for the Diagnosis of COVID-19," *Radiol. Cardiothorac. Imaging*, vol. 2, no. 2, 2020, doi: 10.1148/ryct.2020200196.

[17] A. Borakati, A. Perera, J. Johnson, and T. Sood, "Diagnostic Accuracy of X-Ray versus CT in COVID-19: A Propensity-Matched Database Study," *BMJ Open*, vol. 10, no. 11, Nov. 2020, doi: 10.1136/bmjopen-2020-042946.

[18] Md. M. Islam, F. Karray, R. Alhajj, and J. Zeng, "A Review on Deep Learning Techniques for the Diagnosis of Novel Coronavirus (COVID-19)," *IEEE Access*, vol. 9, pp. 30551–30572, 2021, doi: 10.1109/ACCESS.2021.3058537.

[19] H. Jindal *et al.*, "False-Negative RT-PCR Findings and Double Mutant Variant as Factors of an Overwhelming Second Wave of COVID-19 in India: an Emerging Global Health Disaster," *SN Compr. Clin. Med.*, vol. 3, no. 12, pp. 2383–2388, Dec. 2021, doi: 10.1007/s42399-021-01059-z.

[20] P. Fillatre *et al.*, "A new SARS-CoV-2 variant poorly detected by RT-PCR on nasopharyngeal samples, with high lethality," Infectious Diseases (except HIV/AIDS), preprint, May 2021. doi: 10.1101/2021.05.05.21256690;

[21] Y. H. Jin *et al.*, "A Rapid Advice Guideline for the Diagnosis and Treatment of 2019 Novel Coronavirus (2019-nCoV) Infected Pneumonia (Standard Version)," *Mil. Med. Res.*, vol. 7, no. 1, p. 4, Feb. 2020, doi: 10.1186/s40779-020-0233-6.

[22] F. M. Yener and A. B. Oktay, "Diagnosis of COVID-19 with a Deep Learning Approach on Chest CT Slices," in *2020 Medical Technologies Congress (TIPTEKNO)*, Antalya: IEEE, Nov. 2020, pp. 1–4. doi: 10.1109/TIPTEKNO50054.2020.9299266.

[23] K. Simonyan and A. Zisserman, "Very Deep Convolutional Networks for Large-Scale Image Recognition," *arXiv:1409.1556*, Apr. 2015, Accessed: Dec. 12, 2021. [Online]. Available: http://arxiv.org/abs/1409.1556

[24] F. Chollet, "Xception: Deep Learning With Depthwise Separable Convolutions," in *2017 IEEE Conference on Computer Vision and Pattern Recognition (CVPR)*, Jul. 2017, pp. 1800–1807. doi: 10.1109/CVPR.2017.195.

[25] X. Yang, X. He, J. Zhao, Y. Zhang, S. Zhang, and P. Xie, "COVID-CT-Dataset: A CT Scan Dataset about COVID-19," *arXiv:2003.13865*, Jun. 2020, Accessed: Dec. 12, 2021. [Online]. Available: http://arxiv.org/abs/2003.13865

[26] "Kaggle: Your Machine Learning and Data Science Community." https://www.kaggle.com/ (accessed Jan. 09, 2023).

[27] "ImageNet." https://image-net.org/index.php (accessed Dec. 18, 2021).

[28] X. Wu, Z. Wang, and S. Hu, "Recognizing COVID-19 Positive: Through CT Images," in *2020 Chinese Automation Congress (CAC)*, Shanghai, China: IEEE, Nov. 2020, pp. 4572–4577. doi: 10.1109/CAC51589.2020.9326470.

[29] A. Krizhevsky, I. Sutskever, and G. E. Hinton, "ImageNet Classification with Deep Convolutional Neural Networks," in *Advances in Neural Information Processing Systems*, Curran Associates, Inc., 2012, pp. 1097–1105. [Online]. Available: https://proceedings.neurips.cc/paper/2012/file/c399862d3b9d6b76c8436e924a68c45b-Paper.pdf

[30] K. He, X. Zhang, S. Ren, and J. Sun, "Deep Residual Learning for Image Recognition," *arXiv:1512.03385*, Dec. 2015, Accessed: Dec. 12, 2021. [Online]. Available: http://arxiv.org/abs/1512.03385

[31] F. N. Iandola, S. Han, M. W. Moskewicz, K. Ashraf, W. J. Dally, and K. Keutzer, "SqueezeNet: AlexNet-level accuracy with 50x fewer parameters and <0.5MB model size," *arXiv:1602.07360*, Nov. 2016, Accessed: Dec. 12, 2021. [Online]. Available: http://arxiv.org/abs/1602.07360

[32] G. Huang, Z. Liu, L. van der Maaten, and K. Q. Weinberger, "Densely Connected Convolutional Networks," *arXiv:1608.06993*, Jan. 2018, Accessed: Dec. 12, 2021. [Online]. Available: http://arxiv.org/abs/1608.06993

[33] E. Soares, P. Angelov, S. Biaso, M. H. Froes, and D. K. Abe, "SARS-CoV-2 CT-Scan Dataset: A Large Dataset of Real Patients CT Scans for SARS-CoV-2 Identification," *medRxiv*, 2020, doi: 10.1101/2020.04.24.20078584.

[34] "MNIST handwritten digit database, Yann LeCun, Corinna Cortes and Chris Burges." http://yann.lecun.com/exdb/mnist/ (accessed Jan. 09, 2023).

[35] T. Anwar and S. Zakir, "Deep Learning Based Diagnosis of COVID-19 using Chest CT-Scan Images," in *2020 IEEE 23rd International Multitopic Conference (INMIC)*, Bahawalpur, Pakistan: IEEE, Nov. 2020, pp. 1–5. doi: 10.1109/INMIC50486.2020.9318212.

[36] M. Tan and Q. V. Le, "EfficientNet: Rethinking Model Scaling for Convolutional Neural Networks," *arXiv:1905.11946*, Sep. 2020, Accessed: Dec. 12, 2021. [Online]. Available: http://arxiv.org/abs/1905.11946

[37] S. Wang *et al.*, "A Deep Learning Algorithm Using CT Images to Screen for Corona Virus Disease (COVID-19)," *Eur. Radiol.*, vol. 31, no. 8, pp. 6096–6104, Aug. 2021, doi: 10.1007/s00330-021-07715-1.

[38] C. Szegedy, V. Vanhoucke, S. Ioffe, J. Shlens, and Z. Wojna, "Rethinking the Inception Architecture for Computer Vision," *arXiv:1512.00567*, Dec. 2015, Accessed: Dec. 12, 2021. [Online]. Available: http://arxiv.org/abs/1512.00567

[39] Md. R. Islam and A. Matin, "Detection of COVID 19 from CT Image by the Novel LeNet-5 CNN Architecture," in *2020 23rd International Conference on Computer and Information Technology (ICCIT)*, Dhaka, Bangladesh: IEEE, Dec. 2020, pp. 1–5. doi: 10.1109/ICCIT51783.2020.9392723.

[40] X. He *et al.*, "Sample-Efficient Deep Learning for COVID-19 Diagnosis Based on CT Scans," *medRxiv*, 2020, doi: 10.1101/2020.04.13.20063941.

[41] Md. Foysal and A. B. M. Aowlad Hossain, "COVID-19 Detection from Chest CT Images using Ensemble Deep Convolutional Neural Network," in *2021 2nd International Conference for Emerging Technology (INCET)*, Belagavi, India: IEEE, May 2021, pp. 1–6. doi: 10.1109/INCET51464.2021.9456387.

[42] M. Maftouni, A. C. C. Law, B. Shen, Y. Zhou, N. Ayoobi Yazdi, and Z. Kong, "A Robust Ensemble-Deep Learning Model for COVID-19 Diagnosis based on an Integrated CT Scan Images Database," in *Proceedings of the 2021 IISE Annual Conference and Expo*, Virtual Conference: Institute of Industrial and Systems Engineers (IISE), May 2021, pp. 632–637. [Online]. Available: https://www.proceedings.com/61116.html

[43] "medRxiv.org - the preprint server for Health Sciences." https://www.medrxiv.org/ (accessed Apr. 05, 2023).

[44] "bioRxiv.org - the preprint server for Biology." https://www.biorxiv.org/ (accessed Apr. 05, 2023).

[45] J. P. Cohen, P. Morrison, L. Dao, K. Roth, T. Q. Duong, and M. Ghassemi, "COVID-19 Image Data Collection: Prospective Predictions Are the Future," *arXiv:2006.11988*, Dec. 2020, Accessed: Dec. 12, 2021. [Online]. Available: http://arxiv.org/abs/2006.11988

[46] P. Afshar *et al.*, "COVID-CT-MD: COVID-19 Computed Tomography (CT) Scan Dataset Applicable in Machine Learning and Deep Learning," Sep. 2020, [Online]. Available: http://arxiv.org/abs/2009.14623

[47] S. P. Morozov *et al.*, "MosMedData: Chest CT Scans With COVID-19 Related Findings Dataset," May 2020, [Online]. Available: http://arxiv.org/abs/2005.06465

[48] M. Rahimzadeh, A. Attar, and S. M. Sakhaei, "A Fully Automated Deep Learning-Based Network for Detecting COVID-19 from a New and Large Lung CT Scan Dataset," *Biomed. Signal Process. Control*, vol. 68, p. 102588, Jul. 2021, doi: 10.1016/j.bspc.2021.102588.

[49] M. Jun *et al.*, "COVID-19 CT Lung and Infection Segmentation Dataset." Zenodo, Apr. 2020. doi: 10.5281/ZENODO.3757476.

[50] "COVID-19 CT segmentation dataset," *Medical Segmentation*. https://medicalsegmentation.com/covid19/ (accessed Dec. 12, 2021).

[51] A. G. Howard *et al.*, "MobileNets: Efficient Convolutional Neural Networks for Mobile Vision Applications," *arXiv:1704.04861*, Apr. 2017, Accessed: Dec. 12, 2021. [Online]. Available: http://arxiv.org/abs/1704.04861

[52] "TensorFlow," *TensorFlow*. https://www.tensorflow.org/ (accessed Dec. 12, 2021).

[53] "Keras: the Python deep learning API." https://keras.io/ (accessed Apr. 06, 2023).

[54] "Google Colab." https://colab.research.google.com/ (accessed Dec. 12, 2021).

[55] D. P. Kingma and J. Ba, "Adam: A Method for Stochastic Optimization," *arXiv:1412.6980*, Jan. 2017, Accessed: Dec. 12, 2021. [Online]. Available: http://arxiv.org/abs/1412.6980

[56] H. Panwar, P. K. Gupta, M. K. Siddiqui, R. Morales-Menendez, P. Bhardwaj, and V. Singh, "A deep learning and grad-CAM based color visualization approach for fast detection of COVID-19 cases using chest X-ray and CT-Scan images," *Chaos Solitons Fractals*, vol. 140, p. 110190, Nov. 2020, doi: 10.1016/j.chaos.2020.110190.

[57] M. Dhruv, R. Sai Chandra Teja, R. Sri Devi, and S. Nagesh Kumar, "InRFNet: Involution Receptive Field Network for COVID-19 Diagnosis," *J. Phys. Conf. Ser.*, vol. 2161, no. 1, p. 012064, Jan. 2022, doi: 10.1088/1742-6596/2161/1/012064.

[58] A. Ouahab, "Multimodal Convolutional Neural Networks for Detection of Covid-19 Using Chest X-Ray and CT Images," *Opt. Mem. Neural Netw.*, vol. 30, no. 4, pp. 276–283, Oct. 2021, doi: 10.3103/S1060992X21040044.

[59] A. P. Hartono, C. R. Luhur, C. A. Indriyani, C. R. Wijaya, N. N. Qomariyah, and A. A. Purwita, "Evaluating Deep Learning for CT Scan COVID-19 Automatic Detection," in *2021 International Conference on ICT for Smart Society (ICISS)*, Aug. 2021, pp. 1–7. doi: 10.1109/ICISS53185.2021.9533224.